Electronic Properties of the Trellis-Lattice Hubbard Model: Pseudogap and Superconductivity

Hiroshi Kontani and Kazuo Ueda

Institute for Solid State Physics, University of Tokyo, 7-22-1 Roppongi, Minato-ku, Tokyo 106-8666

(Received 10 March 1998)

We study the electronic states of the two-dimensional frustrated coupled ladder (trellis lattice) Hubbard model, which is a theoretical model of the superconducting material $Sr_{14-x}Ca_xCu_{24}O_{41}$. Temperature dependence of the density of states and magnetic susceptibility are discussed by using the fluctuation exchange method, which is applied to this model for the first time. At half filling, a large pseudogap appears in the density of states at higher temperatures. Moreover, the d-wave superconductivity appears at lower temperatures, where the pseudogap is well developed. These behaviors have similarities to the under-doped high-T_c cuprates. [S0031-9007(98)06461-8]

PACS numbers: 71.27.+a, 71.10.Fd, 74.72.Jt

After the discovery of high-T_c superconductors (HTSC), various copper-oxide compounds have been investigated intensively. In 1996, $Sr_{14-x}Ca_xCu_{24}O_{41}$ was added to the list of a new type of superconductors: For $x = 13.6$, the superconducting transition temperature (T_c) is about 12 K under high pressures, $P \sim 3$ GPa [1]. In $Sr_{14-x}Ca_xCu_{24}O_{41}$, doped holes move on the two-dimensional Cu ($d_{x^2-y^2}$) network, connected by p orbitals of O. The structure of the Cu network is called trellis lattice, which is a frustrated coupled ladders in two dimension as shown in Fig. 1. On the other hand, in HTSC the carrier moves on the square lattice Cu network. For $x = 0$ the system is a Mott insulator, which is represented by the $S = 1/2$ spin Hamiltonian on the trellis lattice. Experimentally, it has a singlet ground state with a spin gap consistent with the theoretical predictions [2]. For $x > 0$, hole carriers are introduced into the trellis lattice, and the resistivity decreases as x increases. For $x = 11.5$, the resistivity shows an anisotropic 2D Fermi liquid behavior ($\rho_a, \rho_c \propto T^2$, $\rho_a/\rho_c \lesssim 15$) for $T > T_c$ under the optimum pressure, $P = 4.5$ GPa [3].

Electronic properties of a single ladder Hubbard model (or t-J model) have been studied intensively by many authors. For example, by exact diagonalization study [4], density matrix renormalization group method [5], resonating-valence-bond (RVB) mean-field theory [6], bosonization technique [7], quantum Monte Carlo (QMC) simulations [8,9], and others. According to these studies, it has been shown that the ground state of a single ladder has an instability towards a d-wave superconductivity. Nonetheless, thermodynamic properties of the two-dimensional trellis lattice Hubbard model, which corresponds to $Sr_{14-x}Ca_xCu_{24}O_{41}$, has not been studied so far. For this model, a perturbation treatment with respect to U is valid at least up to a moderate positive U, which is not the case for 1D systems. Recent perturbative renormalization group study with respect to the interladder coupling and U reports that the 2D Fermi liquid region would be realized for realistic parameters [10].

In this Letter, we study electronic properties of the trellis lattice Hubbard model by using the fluctuation exchange (FLEX) method. Here, we study the metallic state at half filling as the first step, since the frustrating interladder hopping t' stabilizes the paramagnetic metallic state for moderate $U > 0$. As the temperature decreases, a pseudogap appears in the density of states (DOS) below some characteristic temperature T_0, and the uniform magnetic susceptibility χ also begins to decrease below T_0. Successively, a d-wave superconductivity occurs at a critical temperature T_c. We find that $T_c \ll T_0$ and the pseudogap is well developed at T_c. These non-Fermi liquid behaviors of our model, brought by the large spin fluctuations, are also characteristic properties of the HTSC in the small doping region.

The Hubbard Hamiltonian in real space is shown by Fig. 1. The unit cell of this lattice consists of two Cu sites (A,B). We have integrated out the O p-orbital degrees of freedoms. t and t' are the hopping parameters for the intraladder processes and interladder ones, respectively. It is reasonable to assume that $|t| \gg |t'|$ in $Sr_{14-x}Ca_xCu_{24}O_{41}$ because the Cu-O-Cu bond angle is close to 180° within each ladder, but nearly 90° between ladders. U is the on-site Coulomb repulsion. In this Letter, we put $t = -1$ and $t' = -0.15$, which is consistent with the recent band calculation [11]. The noninteracting band width D is given by $D = 6|t| + 4|t'| = 6.6$. Figure 2 shows the two Fermi surfaces, both are electronlike and open orbits.

In the present study we use the FLEX method, which is a kind of self-consistent perturbation theory with

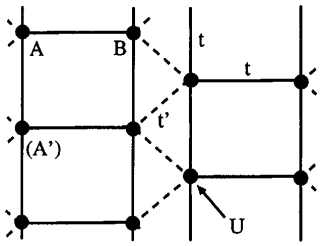

FIG. 1. Trellis lattice Hubbard model. The length of t bonds and t' bonds are 1 and $1/\sqrt{2}$, respectively.

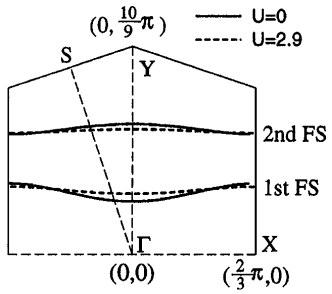

FIG. 2. One-half of the Brillouin zone. Fermi surfaces at half filling are shown by the solid lines for $U = 0$ and by the dashed lines for $U = 2.9$. In both cases, $t = -1$, $t' = -0.15$, and $T = 0.02$.

respect to U. The FLEX method has advantages for handling large spin fluctuations. It has been applied to HTSC by many authors, and various non-Fermi liquid behaviors observed in HTSC are reproduced well [12–15]. Though it is an approximation, it has been shown that the imaginary time Green's function obtained by the FLEX agrees well with the QMC result for the square lattice Hubbard model with moderate U [12]. In our calculation, both the thermal Green's function and the self-energy have a 2×2 matrix form, i.e., $G_{\alpha\beta}(\mathbf{k}, \epsilon_n)$ and $\Sigma_{\alpha\beta}(\mathbf{k}, \epsilon_n)$, where $\alpha, \beta = A$ or B. The Dyson equation is written as

$$\{\hat{G}(\mathbf{k}, \epsilon_n)\}^{-1} = \{\hat{G}^0(\mathbf{k}, \epsilon_n)\}^{-1} - \hat{\Sigma}(\mathbf{k}, \epsilon_n), \qquad (1)$$

where $\hat{G}^0(\mathbf{k}, \epsilon)$ is the unperturbed Green's function. The self-energy is given by

$$\Sigma_{\alpha\beta}(\mathbf{k}, \epsilon_n) = T \sum_{\mathbf{q},l} G_{\alpha\beta}(\mathbf{k} - \mathbf{q}, \epsilon_n - \omega_l) \cdot U^2 \times \left[\frac{3}{2} \hat{\chi}^{(-)}(\mathbf{q}, \omega_l) + \frac{1}{2} \hat{\chi}^{(+)}(\mathbf{q}, \omega_l) - \hat{\chi}^0(\mathbf{q}, \omega_l) \right]_{\alpha\beta}, \qquad (2)$$

$$\hat{\chi}^{(\pm)}(\mathbf{q}, \omega_l) = \hat{\chi}^0 \cdot \{\hat{1} \pm U\hat{\chi}^0(\mathbf{q}, \omega_l)\}^{-1}, \qquad (3)$$

$$\chi^0_{\alpha\beta}(\mathbf{q}, \omega_l) = -T \sum_{\mathbf{k},n} G_{\alpha\beta}(\mathbf{q} + \mathbf{k}, \omega_l + \epsilon_n) G_{\beta\alpha}(\mathbf{k}, \epsilon_n), \qquad (4)$$

where $\epsilon_n = (2n + 1)\pi T$ and $\omega_l = 2l\pi T$, respectively. The $\mathbf{k}$ summation is taken in the first Brillouin zone, shown in Fig. 2. We solve Eqs. (1)–(4) self-consistently, choosing the chemical potential μ so as to keep the total electron number constant. We use 4096 $\mathbf{k}$-points and ~512–2048 Matsubara frequencies for $T \geq 0.02$. ($|t| = 1$.)

Now, we show the results of the present FLEX calculations. Figure 3(a) shows the DOS $\rho(\omega)$ as a function of energy for various U, and Fig. 3(b) shows the DOS at μ as a function of U, at $T = 0.02$ in both cases. Hereafter we take μ as the origin of energy. It should be noted that our model is particle-hole asymmetric when

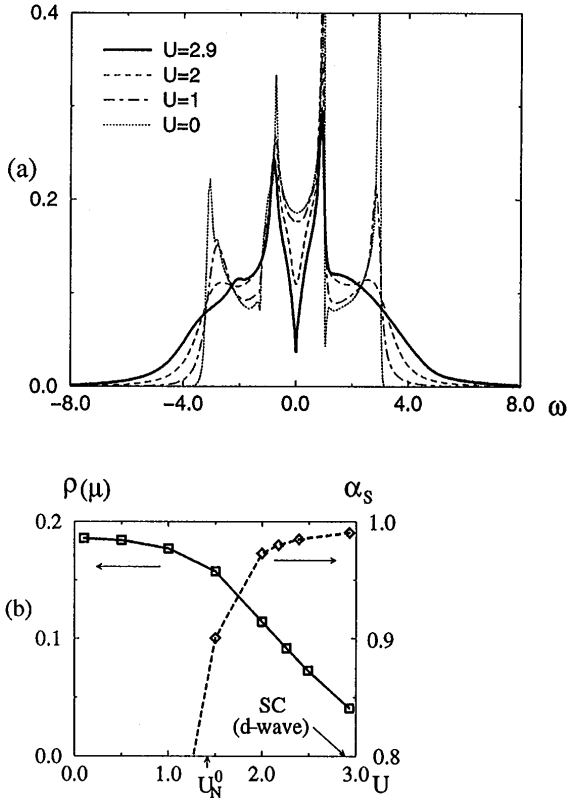

FIG. 3. (a) The DOS as a function of energy for several $U \geq 0$. (b) The DOS at μ (solid line) and the Stoner factor α_S (dashed line) as a function of U, at $T = 0.02$.

$t' \neq 0$. By definition, the DOS is given by $\rho(\omega) = (-2/\pi)\sum_{\mathbf{k}} \mathrm{Im}\, G_{AA}(\mathbf{k}, \omega + i0)$, and $G_{AA}(\mathbf{k}, \omega + i0)$ is obtained through numerical analytic continuation from $G_{AA}(\mathbf{k}, \epsilon_n)$ by N-point Padé approximation [16].

We see in Fig. 3 that a V-shape pseudogap around μ grows monotonously as U increases. This is very different from the results obtained by the dynamical mean field theory since the DOS at μ does not change by the latter method. Based on the extrapolation from the normal state, the metal-insulator (MI) transition may take place around $U = U_c \sim 3.5$. By neglecting the vertex corrections, the Stoner factor of the present model α_S is defined as

$$\alpha_S = \max_{\mathbf{k}} \{U \cdot [\chi_{AA}(\mathbf{k}, \omega = 0) + |\chi_{AB}(\mathbf{k}, \omega = 0)|]\}, \qquad (5)$$

which is given at $(0, \pi)$ in case of half filling. $\alpha_S < 1$ is satisfied at least for $U \leq 2.9$ in the FLEX approximation, which means there is no magnetic ordering. On the other hand, in the RPA calculation without the self-consistency condition, $\alpha_S \geq 1$ for $U \geq U_N^0 = 1.4$. In the FLEX calculation, the DOS at μ begins to decrease monotonously for $U \geq U_N^0$, which may be interpreted that large quantum fluctuations prevent the magnetic instability by making a pseudogap. As U is increased further, we find that the d-wave superconductivity occurs for $U \geq 2.9$, where the system is close to the magnetic critical point, $\alpha_S \sim 0.99$.

We determine T_c by solving the linearized Eliashberg equation with respect to the singlet-pairing order parameter, $\phi_{\alpha\beta}(-\mathbf{k}, \epsilon_n) = +\phi_{\beta\alpha}(\mathbf{k}, \epsilon_n)$,

$$\lambda\phi_{\alpha\beta}(\mathbf{k}, \epsilon_n) = -T\sum_{\mathbf{q},m}\sum_{\alpha',\beta'} V_{\alpha\beta}(\mathbf{k} - \mathbf{q}, \epsilon_n - \epsilon_m)G_{\alpha\alpha'}(\mathbf{q}, \epsilon_m)G_{\beta\beta'}(-\mathbf{q}, -\epsilon_m)\phi_{\alpha'\beta'}(\mathbf{q}, \epsilon_m)\,,$$
$$\hat{V}(\mathbf{k}, \omega_l) = \frac{3}{2}U^2\hat{\chi}^{(-)}(\mathbf{k}, \omega_l) - \frac{1}{2}U^2\hat{\chi}^{(+)}(\mathbf{k}, \omega_l) + U\,, \tag{6}$$

where T_c is given by the condition that $\lambda = 1$. We find that $T_c \approx 0.02$ for the present set of parameters. To identify the symmetry of the superconductivity the nearest neighbor pairing functions [$\Delta_{AA'} = \mathrm{Re}\sum_{\mathbf{k}} \phi_{AA}(\mathbf{k}, i\epsilon_n \to 0)\exp(ik_y)$ and $\Delta_{AB} = \mathrm{Re}\sum_{\mathbf{k}} \phi_{AB}(\mathbf{k}, i\epsilon_n \to 0)\exp(ik_x)$] are calculated (see Fig. 1.) We have found that $\Delta_{AA'}\Delta_{AB} < 0$ and $|\Delta_{AB}|/|\Delta_{AA'}| = 1.4$, which means that a d-wave type superconductivity is realized. We have also looked at a triplet-pairing solution [$\phi_{\alpha\beta}(-\mathbf{k}, \epsilon_n) = -\{\phi_{\alpha\beta}(\mathbf{k}, \epsilon_n)\}^*$] by solving the corresponding linearized Eliashberg equation, but the T_c^{triplrt} is always lower than T_c^{singlet}. It has been confirmed that t' dependence of T_c is very weak. Even at half filling, the superconducting state is stable against magnetic ordering, which is consistent with the fact that the trellis lattice spin system has the gapful spin singlet ground state.

Figure 4(a) shows the DOS as a function of energy for various T, and Fig. 4(b) the DOS at μ as a function of T, for $U = 2.9$ in both cases. As the temperature decreases, the V-shape pseudogap around μ grows monotonously below the characteristic temperature, $T_0 \sim 0.4$. The size of the V-shape pseudogap, measured from the width between the two peaks, is $\Delta_{\mathrm{pg}} \sim 2$. Interestingly, Δ_{pg} is about 5 times larger than T_0 for the present set of parameters. At $T_c \approx 0.02$, the d-wave superconductivity occurs as was discussed in the preceding paragraph.

The pseudogap behavior in our model, calculated by the FLEX method, has close relationship to the spin fluctuations. It is a characteristic feature of the present model that the pseudogap behavior is observed for a wide region of parameters, U or T. Similarly, the square lattice Hubbard model at half filling also shows the pseudogap behavior as a precursor of the MI transition in the FLEX study [15]. However, a clear pseudogap develops only at close vicinity of the magnetic critical point, where $(1 - \alpha_S)^{-1} \gg O(100)$. We find that the critical region is much wider for the trellis lattice than for the square lattice. Moreover, superconductivity is not realized in the square lattice model at half filling prevented by magnetic ordering.

Now, we investigate the temperature dependence of the magnetic susceptibilities. In Fig. 5, we show the uniform magnetic susceptibility (χ) and the local magnetic susceptibility of the nearest neighbor sites in a ladder ($\chi_{AA'}$, χ_{AB}). They are derived, neglecting the vertex corrections, as follows: $\chi = \lim_{\mathbf{k}\to 0}\mu_B \times \{\chi_{AA}^{(-)}(\mathbf{k}, 0) + \chi_{AB}^{(-)}(\mathbf{k}, 0)\}$, $\chi_{AA'} = \mu_B\sum_{\mathbf{k}}\chi_{AA}^{(-)}(\mathbf{k}, 0) \times \exp(ik_x)$, and $\chi_{AB} = \mu_B\sum_{\mathbf{k}}\chi_{AB}^{(-)}(\mathbf{k}, 0)\exp(ik_y)$. In Fig. 5, we see that χ shows a maximum around $T_0 \sim 0.4$, which corresponds to the temperature of the pseudogap formation (see Fig. 4). Moreover, both $\chi_{AA'}$ and χ_{AB}

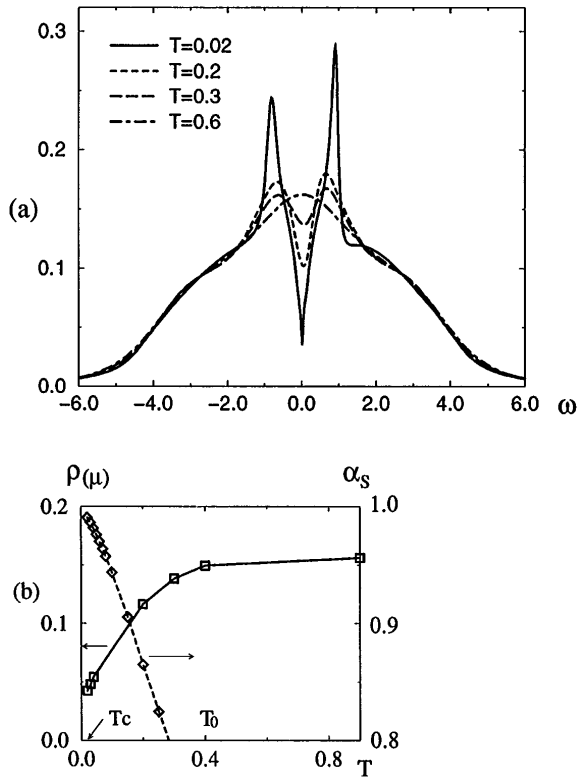

FIG. 4. (a) The DOS as a function of energy for several $T \geq 0.02$. (b) The DOS at μ (solid line) and the Stoner factor α_S (dashed line) as a function of T ($U = 2.9$).

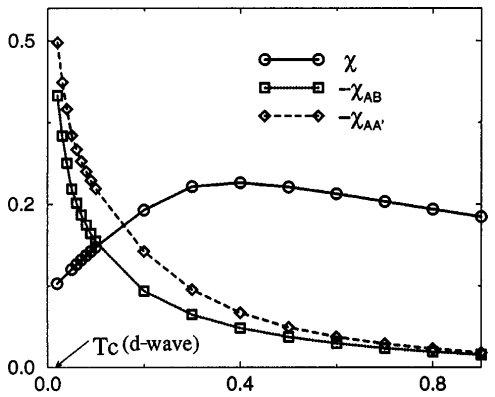

FIG. 5. The uniform magnetic susceptibility χ and the local magnetic susceptibility of the nearest neighbors $\chi_{AA'}$ and χ_{AB}, as a function of T ($U = 2.9$). We put $\mu_B = 1$.

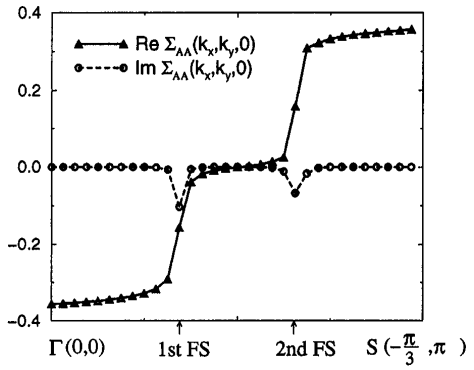

FIG. 6. **k** dependence of the diagonal part of the self-energy $\Sigma_{AA}(k_x, k_y, \omega = 0)$.

grow rapidly as the temperature decreases, which means the increase of short range singlet correlations at lower temperatures. To be precise, for the calculation of correlation functions, the vertex corrections are indispensable to satisfy conservation laws [17]. In general, the Stoner factor α_S defined by Eq. (5) is slightly overestimated, especially at low temperatures [14]. In the same way, the obtained $\chi_{AA'}$ and χ_{AB} at lower temperatures would be overestimated, although the qualitative behavior is expected to be the same.

Next, we discuss the origin of the pseudogap behaviors. Figure 6 shows $\Sigma_{AA}(\mathbf{k}, \omega = \mu)$ at $T = 0.02$ along the Γ point to the S point (see Fig. 2). One remarkable feature is that the **k** dependence of the real part is large at the Fermi surface, which reduces the quasiparticle effective mass. On the other hand, its ω dependence is rather moderate. Another remarkable point is that the absolute value of the imaginary part is much larger than the temperature. In this sense, the normal state just above T_c is an incoherent metallic state. These two characters are the origin of the pseudogap behavior of our model.

It is also interesting to discuss the shape of the Fermi surfaces. Figure 2 shows the Fermi surfaces at $T = 0.02$ for $U = 0$ and $U = 2.9$. They are defined by Re $G_{\alpha\beta}(\mathbf{k}, \omega = \mu) = 0$. Although the position does not change so much, the dispersion is drastically changed due to the interaction, which may have intimate relation to various non-Fermi liquid behaviors of the present model. For $U = 2.9$, the nesting feature of the Fermi surfaces is enhanced clearly. It means that the effective interladder coupling t'^* is renormalized to a smaller value by the correlation effect. In other words, the hopping processes between ladders are suppressed in the interacting case. We point out that the nesting tendency of the interacting Fermi surface is also observed in the square lattice model [13].

Finally, we discuss some experimental results of $Sr_{14-x}Ca_xCu_{24}O_{41}$. The angle resolved photoemission experiments [18] show the absence of DOS at μ at $T = 130$ K. This is consistent with the pseudogap formation predicted by the present work since the pseudogap survives the doping into the present model [19]. Moreover, the enhancement of anisotropy of the resistivity at low temperatures experimentally observed [3] may be explained in terms of the renormalization of the effective t'^*. Another consequence of the large pseudogap formation derived by the present work is that the electronic states will be unstable against the localization effect by impurities, or the CDW transition. In fact, at low temperatures good metallic states are realized experimentally only in the high-doping region [1,3]. This sensitivity to impurity scatterings may be the reason of low T_c in $Sr_{14-x}Ca_xCu_{24}O_{41}$, compared with the HTSC.

In summary, we have studied low temperature electronic properties of the trellis lattice Hubbard model at half filling by using the FLEX method, for moderate U ($U \sim 2.9$). As the temperature is lowered, a pseudogap emerges in the DOS suppressing magnetic orderings, with increasing short range singlet correlations. As T is lowered further, we find a d-wave superconductivity at $T_c \approx 0.02$ in the present model. The large pseudogap formation seems to reduce T_c, in spite of the strong short range singlet correlations. On the other hand, in the square lattice model, magnetic instability prevents the occurrence of superconductivity at half filling. It is remarkable that the geometry of the trellis lattice makes these pseudogap properties more explicit than in the square lattice model.

We are grateful to T. Moriya and K. Yamada for useful comments and encouragement. We also thank N. Môri, K. Yonemitsu, J. Kishine, T. Takimoto, and S. Koikegami for valuable comments and discussions. This work is financially supported by a Grant-in-Aid for Scientific Research on Priority Areas from the Ministry of Education, Science, Sports and Culture.

[1] M. Uehara *et al.*, J. Phys. Soc. Jpn. **65**, 2764 (1996).
[2] E. Daggoto and T. M. Rice, Science **47**, 618 (1996).
[3] T. Nagata *et al.*, Physica (Amsterdam) **282C–287C**, 153 (1997).
[4] E. Daggoto *et al.*, Phys. Rev. B **45**, 5744 (1992).
[5] R. M. Noack *et al.*, Phys. Rev. Lett. **73**, 882 (1994).
[6] M. Sigrist *et al.*, Phys. Rev. B **49**, 12 058 (1994).
[7] L. Balents and M. P. A. Fisher, Phys. Rev. B **53**, 12 133 (1996).
[8] K. Kuroki *et al.*, Phys. Rev. B **54**, 15 641 (1996).
[9] T. Dahm and D. J. Scalapino, Physica (Amsterdam) **288C**, 33 (1997).
[10] J. Kishine and K. Yonemitsu, J. Phys. Soc. Jpn. **66**, 3725 (1997).
[11] M. Arai and H. Tsunetsugu, Phys. Rev. B **56**, 4305 (1997).
[12] N. E. Bickers *et al.*, Phys. Rev. Lett. **62**, 961 (1989).
[13] P. Monthoux and D. Pines, Phys. Rev. B **47**, 6069 (1993).
[14] T. Dahm and L. Tewordt, Phys. Rev. B **52**, 1297 (1995).
[15] J. J. Deisz *et al.*, Phys. Rev. Lett. **76**, 1312 (1996).
[16] H. J. Vidberg and J. W. Serene, J. Low Temp. Phys. **19**, 179 (1977).
[17] G. Baym and L. P. Kadanoff, Phys. Rev. **124**, 287 (1961).
[18] T. Takahashi *et al.*, Phys. Rev. B **56**, 7870 (1997).
[19] H. Kontani and K. Ueda (unpublished).